

SGOR: Outlier Removal by Leveraging Semantic and Geometric Information for Robust Point Cloud Registration

Guiyu Zhao, Zhentao Guo, and Hongbin Ma, *Senior Member, IEEE*

Abstract—In this paper, we introduce a new outlier removal method that fully leverages geometric and semantic information, to achieve robust registration. Current semantic-based registration methods only use semantics for point-to-point or instance semantic correspondence generation, which has two problems. First, these methods are highly dependent on the correctness of semantics. They perform poorly in scenarios with incorrect semantics and sparse semantics. Second, the use of semantics is limited only to the correspondence generation, resulting in bad performance in the weak geometry scene. To solve these problems, on the one hand, we propose secondary ground segmentation and loose semantic consistency based on regional voting. It improves the robustness to semantic correctness by reducing the dependence on single-point semantics. On the other hand, we propose semantic-geometric consistency for outlier removal, which makes full use of semantic information and significantly improves the quality of correspondences. In addition, a two-stage hypothesis verification is proposed, which solves the problem of incorrect transformation selection in the weak geometry scene. In the outdoor dataset, our method demonstrates superior performance, boosting a 22.5 percentage points improvement in registration recall and achieving better robustness under various conditions. Our code is available.

I. INTRODUCTION

As an important task in 3D vision, point cloud registration has a wide range of applications, such as simultaneous localization and mapping [1]–[4], robot grasping [5], [6], etc. There are many methods for point cloud registration, among which the most mainstream is the correspondence-based point cloud registration [7]–[10]. The correspondence-based method obtains a set of correspondences through feature extraction and matching, and then the transformation is estimated through SVD or RANSAC [11]. However, the effectiveness of this method is heavily contingent on the quality of correspondences, particularly in scenarios characterized by low overlap, large scenes, and sparse features. Therefore, removing outliers to filter correspondences becomes a critical step in achieving robust and accurate registration.

In recent years, research in outlier removal for point cloud registration has gained significant momentum. This research can be categorized into two main approaches: learning-based methods and traditional geometric methods. PointDSC [12] enhances spatial consistency within features through neural networks, resulting in correspondences of higher quality.

This work was partially funded by the National Key Research and Development Plan of China (No. 2018AAA0101000) and the National Natural Science Foundation of China under grant 62076028 (Corresponding author: Hongbin Ma)

Guiyu Zhao, Zhentao Guo, and Hongbin Ma are with the National Key Lab of Autonomous Intelligent Unmanned Systems, School of Automation, Beijing Institute of Technology, 100081, Beijing, P. R. China (e-mail: 3120220906@bit.edu.cn, zt.guo1230@163.com, mathmhb@bit.edu.cn).

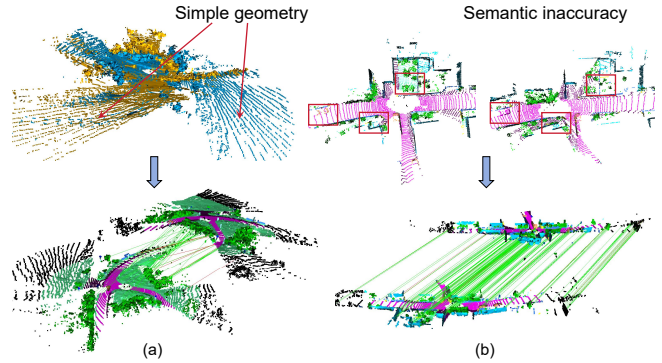


Fig. 1. Our method can also achieve robust registration even in the case of simple geometry and semantic inaccuracy. The green line is the correct correspondence and the red line is the wrong correspondence.

SC2-PCR [13] introduces second-order spatial geometric consistency, notably enhancing the effectiveness of outlier removal. MAC [14] incorporates the maximal clique of graph theory into point cloud registration, leading to more accurate registration. However, all these methods primarily focus on outlier removal by better capturing geometric consistency. These geometric-only methods perform poorly in flat, simple scenarios with lots of roads, streets, etc.

With the progress of semantic segmentation research [15], it has a great prospect to promote the improvement of other computer vision tasks. It is a good idea to use semantic information [1], [16] to improve geometry-only methods, which solves the problem of insufficient geometric information. However, they all have some defects, leading to failure in robust registration. **First**, Segregator [1] conducts instance-level semantic clustering and Pagor [16] uses point-to-point semantic judgment. Both of them are highly dependent on the accuracy of semantic segmentation, and semantics error of the point will seriously affect the final result. **Second**, Their use [1], [16] of semantics only is limited to correspondence generation, and the outlier removal and hypothesis verification are still only based on geometry, which suffers from the same problems as geometric-only methods. As shown in Fig. 1, our method solves these two problems.

In this paper, we propose a new method of using geometric and semantic information to achieve robust registration. **On the one hand**, we propose secondary ground segmentation and loose semantic consistency based on regional voting, which reduces the dependence on semantic accuracy and is more robust to semantic errors. **On the other hand**, we make full use of semantic prior information through semantic-geometric consistency and two-stage hypothesis verification

based on the ground prior and solve the problem that the previous semantic-based methods [1], [16] still rely heavily on geometric information in outlier removal and hypothesis verification. Therefore, this enables our method to achieve robust registration in the face of geometrically deficient scenarios (large areas of ground). Our method performs best in the outdoor dataset, achieving more robust registration.

- We propose a new semantic-based idea to complete point cloud registration, which achieves robust registration with a 22.5 pp improvement in registration recall.
- By using secondary ground segmentation and loose regional semantic consistency, our method is more robust to semantic accuracy and richness.
- With the semantic-geometric consistency and verification based on ground prior, we fully leverage semantics in the outlier removal and hypothesis verification, solving the problem in the scenarios with weak geometry.

II. RELATED WORK

A. Outlier Removal for Point Cloud Registration

Random Sampling Consensus (RANSAC) [11], [17], as a classical and effective correspondence estimation method, is also widely used today. However, it is difficult to converge when there are a large number of outliers. To address this challenge, a lot of works [12]–[14], [18]–[21] have been dedicated to outlier removal through geometric invariants. FGR [18] leverages the Geman-McClure cost to transform non-convex problems into convex ones, resulting in a significant enhancement of correspondence quality. DGR [19] employs convolutional networks to predict the confidence levels of correspondences. PointDSC [12] introduces a spatial non-local consistency module that incorporates geometric consistency into features, subsequently filtering out outliers. GeoTransformer [22] utilizes a local-to-global registration module, providing an effective way for refining correspondences and achieving robust registration. SC2-PCR [13] introduces second-order spatial geometric consistency, leading to substantial improvements in outlier removal performance. Additionally, MAC [14] introduces the maximal clique concept into point cloud registration, resulting in significant enhancements. However, These methods primarily focus on the utilization of geometric invariants for outlier removal while neglecting the significance of semantic priors, leading to not robust registration under the condition of simple geometric structures and sparse features.

B. Semantics for Enhancing Computer Vision Tasks

With the development of deep learning and the proposal of foundation models [23], [24], semantic segmentation tasks have developed rapidly. Using semantics as a prior to assist other computer vision tasks has become an efficient way. Previously, there has been a lot of work using semantic information for 3D reconstruction and SLAM. Menini et al. [25] use a deep learning-based method to introduce semantics into TSDF and improve the effect of indoor 3D reconstruction. Huang et al. [26] establish a semantic pose graph using semantic priors to achieve globally consistent

3D reconstruction. SuMa++ [27] combines semantics into surfel-based mapping and then performs semantic ICP, which achieves the best performance in outdoor highway scenes. Segregator [1] uses semantic and geometric information to cluster points into instance clusters, and match the instance clusters to achieve point cloud registration. Qiao et al. [16] use a pyramid semantic graph and cascaded gradient ascend method to achieve global registration. In the past two years, these few studies [1], [16] have introduced semantics into point cloud registration, and have achieved certain improvements, but there are many problems such as a narrow range of applicable scenarios and insufficient use of semantic information.

III. METHODOLOGY

A. Problem Formulation

Given two point clouds $\mathbf{P} = \{\mathbf{p}_i \in \mathbb{R}^3 \mid i = 1, \dots, I\}$ and $\mathbf{Q} = \{\mathbf{q}_j \in \mathbb{R}^3 \mid j = 1, \dots, J\}$ with overlapping regions, point cloud registration is to align these two point clouds \mathbf{P} and \mathbf{Q} by a transformation $\mathbf{T} = \{\mathbf{R}, \mathbf{t}\}$ where $\mathbf{R} \in SO(3)$ and $\mathbf{t} \in \mathbb{R}^3$. Furthermore, in correspondence-based methods, the correspondence set \mathcal{I} is acquired through feature matching. Subsequently, these methods seek to determine the transformation \mathbf{T} that minimizes the Euclidean distance between each point \mathbf{p}_i in the transformed point cloud $\mathbf{T}(\mathbf{P})$ and its corresponding point \mathbf{p}_j in the point cloud \mathbf{Q}

$$\arg \min_{\mathbf{R} \in SO(3), \mathbf{t} \in \mathbb{R}^3} \sum_{(\mathbf{p}_i, \mathbf{q}_j) \in \mathcal{I}} \|\mathbf{R} \cdot \mathbf{p}_i + \mathbf{t} - \mathbf{q}_j\|_2^2 \quad (1)$$

where this problem is usually solved by SVD. However, the effectiveness of this approach is heavily contingent on the accuracy of the correspondences. To enhance the accuracy of registration, we perform outlier removal to get a subset of more reliable correspondences \mathcal{I}' , where $\mathcal{I}' \subseteq \mathcal{I}$. The overall framework of our approach is shown in Fig. 2.

B. Semantic-aware Correspondence Establishment

In the feature-based registration method, descriptors such as fast point feature histograms (FPFH) [28] and fully convolutional geometric features (FCGF) [29] are extracted for feature matching. However, especially in scenarios with indistinct features, the inlier ratio of correspondences is quite low, leading to non-robust registration. Furthermore, in the case of large outdoor scenes, a significant portion of the point cloud is occupied by points on the ground and road, which have indistinct features and limited discriminative capability. This leads to a significant challenge to establishing correspondences. To address these issues, we propose the semantic-aware correspondence establishment approach.

Semantic-geometric space. First, we acquire the semantic label s_i of each point \mathbf{p}_i through the mature semantic segmentation method [15] or directly using the semantic priors. By combining the 3D coordinates and semantic labels, a semantic-geometric space denoted as $\mathbb{U} = \mathbb{R}^3 \times \mathbb{S}$ is created, where \mathbb{S} represents the set of all possible semantic labels. The semantic point cloud $\mathbf{U} \subseteq \mathbb{U}$ serves as the input of our method where semantic point $(\mathbf{p}_i, s_i) \in \mathbf{U}$.

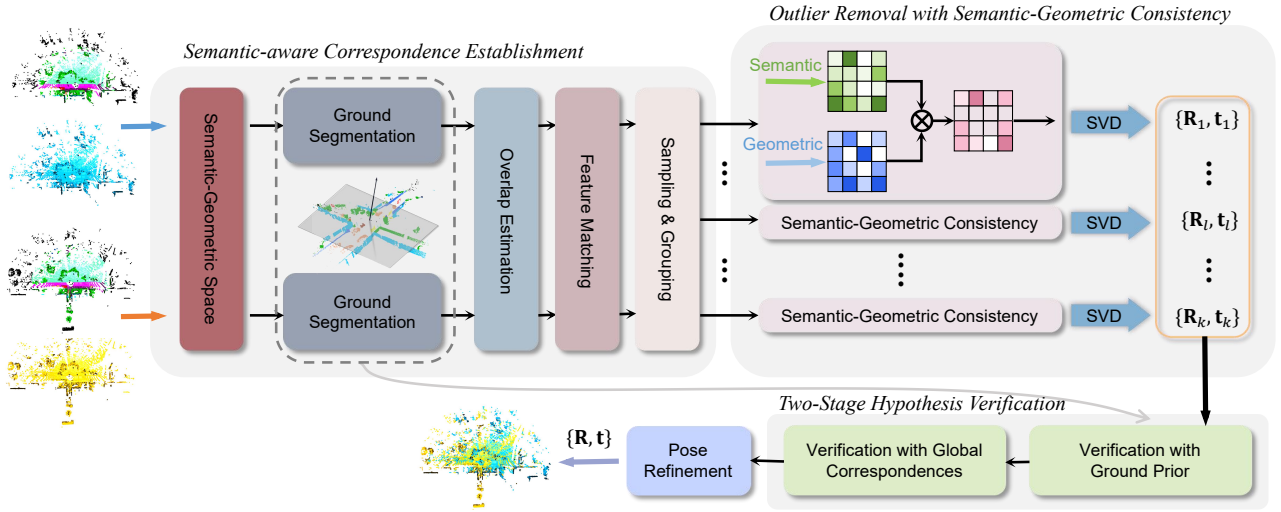


Fig. 2. Pipeline of our proposed method. First, we input the point cloud and its semantics to construct a semantic-geometric space \mathcal{U} . Next, the secondary ground segmentation separates the point cloud into ground \mathcal{U}_{P_g} and non-ground points \mathcal{U}_{P_n} . Subsequently, we estimate the overlap region \mathcal{S}_{P_g} within the semantic space, extract point features for feature matching, and establish the correspondences \mathcal{G} . After that, we obtain local correspondences \mathcal{G}^k by sampling and grouping. Outliers within each local correspondence are filtered based on semantic-geometric consistency, and local transformations \mathbf{T}_l are estimated. Finally, the optimal transformation $\hat{\mathbf{R}}$ is selected through the two-stage hypothesis verification.

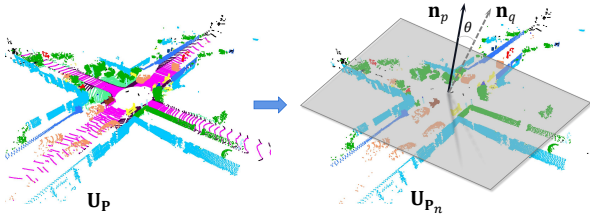


Fig. 3. Ground segmentation and verification with ground prior.

Secondary ground segmentation. We represent the set of semantic labels pertaining to ground and road as S_g , while the set of labels for non-ground points is denoted as $S_n = \overline{S_g}$. By using semantic labels, we partition the semantic point cloud \mathcal{U}_P into ground point clouds \mathcal{U}_{P_g} and non-ground point clouds \mathcal{U}_{P_n} as follows:

$$\mathcal{U}_{P_g} = \{(\mathbf{p}_i, s_i) | s_i \in S_g, \forall (\mathbf{p}_i, s_i) \in \mathcal{U}\}. \quad (2)$$

However, this segmentation method is highly dependent on single-point semantics. To mitigate the influence of semantic errors of points, we conduct a secondary verification. We employ a simple SVD to extract planes $ax + by + cz + d = 0$ from ground points \mathcal{U}_{P_g} . Subsequently, we utilize the Euclidean distance from each point to the plane for secondary segmentation and new ground points \mathcal{U}_{P_g} meet the following conditions:

$$\frac{|a\mathbf{p}_i(x) + b\mathbf{p}_i(y) + c\mathbf{p}_i(z) + d|}{a^2 + b^2 + c^2} < \sigma_g \quad (3)$$

where σ_g is a distance threshold. Then, we use SVD again on the new ground points \mathcal{U}_{P_g} to update the ground normal $\mathbf{n}_p \leftarrow (a', b', c')$. This module helps reduce the reliance on single-point semantic information entirely. It not only enhances processing efficiency by reducing the number of

ground points but also filters out ground points with indistinctive features, thereby facilitating feature matching. Moreover, we also harness the ground normal \mathbf{n}_p as a robust prior for guiding hypothesis verification in Section III-D.

In contrast to [10] using the cross-attention mechanism to achieve overlap region estimation, we obtain the intersection \mathcal{S}_o of the semantic sets \mathcal{S}_{P_n} and \mathcal{S}_{Q_n} within the semantic space and then screen out the semantic overlap region

$$\begin{aligned} \mathcal{U}_{P_o} &= \{(\mathbf{p}_i, s_i) | s_i \in \mathcal{S}_{P_n} \cap \mathcal{S}_{Q_n}, \forall (\mathbf{p}_i, s_i) \in \mathcal{U}\}, \\ \mathcal{U}_{Q_o} &= \{(\mathbf{q}_i, s_i) | s_i \in \mathcal{S}_{P_n} \cap \mathcal{S}_{Q_n}, \forall (\mathbf{q}_i, s_i) \in \mathcal{U}\}. \end{aligned} \quad (4)$$

Correspondences grouping. We obtain the initial correspondences \mathcal{G} by feature matching using FPFH (or FCGF) descriptor on the non-ground points. Different from [1], which directly clusters the correspondences into single-instance correspondences according to the semantic label, we use sampling and grouping methods to cluster the correspondence. The clustered correspondences contain multiple semantic labels, which is more robust to semantic errors and more suitable for semantic consistency. First, correspondences \mathcal{G} is sampled through spectral matching [30] to get L key correspondences \mathcal{G}^k , and then k-nearest neighbor (kNN) search is conducted on \mathcal{G}^k based on source points to get L sets of local correspondences \mathcal{G}_l where $\mathcal{G}_l, l = 1, \dots, L$.

C. Outlier Removal with Semantic-Geometric Consistency

Despite the initial optimization of correspondences, a considerable number of mismatches still persist. In this section, a semantic-geometric double consistency criterion is proposed to eliminate mismatches.

For local correspondences \mathcal{G}_l , geometric consistency matrix, and semantic consistency matrix are calculated respectively. For geometric consistency, we choose the transformation invariant of Euclidean space, the point pair distance, as

the geometric consistency score d_{ij} of one correspondence.

$$d_{ij} = \left| \|\mathbf{p}_i - \mathbf{p}_j\|_2 - \|\mathbf{q}_i - \mathbf{q}_j\|_2 \right| \quad (5)$$

This score d_{ij} is zeroed by giving a distance threshold σ_d . We get a local geometric consistency matrix $\mathbf{M}^g = [m_{ij}^g]_{k \times k}$

$$m_{ij}^g = \mathbf{1} \left(\frac{d_{ij}^2}{\sigma_d^2} - 1 \leq 0 \right) \quad (6)$$

where i and j are the indices of correspondences \mathcal{G}_l , and k is the number of correspondences in \mathcal{G}_l . $\mathbf{1}(\cdot)$ is the indicator function. To overcome the vulnerability of local regions to outliers, we use the global geometric consistency information to guide the selection of local correspondences. Therefore, we calculate the local-to-global geometric consistency matrix $\mathbf{M}' = [m'_{ij}]_{k \times w}$ where i is the index of correspondences \mathcal{G}_l , j is the index of correspondences \mathcal{G} , and w is the size of the correspondences \mathcal{G} . Finally, we obtain the global-aware local geometric consistency matrix \mathbf{M}_g^*

$$\mathbf{M}_g^* = \mathbf{M}_g \circ \left(\mathbf{M}'_g \mathbf{W}_m \mathbf{M}'_g{}^\top \right) \quad (7)$$

where operator \circ represents the element-wise product and $\mathbf{W}_m = [w'_{ij}]_{w \times w}$ is the weight matrix of the consistency between correspondences, calculated as

$$w'_{ij} = \exp\left(-\frac{d_{ij}^2}{2\sigma_d^2}\right). \quad (8)$$

With this distance weight \mathbf{W}_m , our geometric consistency matrix is more robust to anomalous correspondences.

Analysis: Geometric meaning of Matrix \mathbf{M}_g^* . *The element in matrix \mathbf{M}'_g represents the consistency between a correspondence in \mathcal{G}_l and a correspondence in \mathcal{G} . In cases where all weights \mathbf{W}_m are equal to 1, \mathbf{M}'_g undergoes direct multiplication with $\mathbf{M}'_g{}^\top$, resulting in elements that denote the count of correspondences in \mathcal{G} exhibiting consistency with two correspondences from \mathcal{G}_l . Subsequently, through element-wise multiplication with \mathbf{M}_g , the score of correspondences in \mathcal{G}_l that fail to meet the consistency criteria is set to 0. In this case, the matrix quantifies the score of consistency achieved by the two sets of correspondences \mathcal{G}_l within the global correspondences \mathcal{G} . By introducing distance weights, correspondences that are distant from correspondences \mathcal{G}_l are assigned lower weights, thereby enhancing their resistance to the influence of noise.*

Relying solely on geometric consistency may result in poor performance when confronted with a singular geometric structure of the actual scene, such as open roads or orderly blocks, leading to incorrectly filtering correspondences. To address this issue and achieve more robust registration, we introduce semantic consistency. By comparing whether the semantics of the correspondences are the same, we obtain a tight semantic consistency matrix of correspondences \mathcal{G}_l

$$\mathbf{M}_s = \begin{bmatrix} (s_1^p, s_1^p) \odot (s_1^q, s_1^q) & \cdots & (s_1^p, s_k^p) \odot (s_1^q, s_k^q) \\ \vdots & \ddots & \vdots \\ (s_k^p, s_1^p) \odot (s_k^q, s_1^q) & \cdots & (s_k^p, s_k^p) \odot (s_k^q, s_k^q) \end{bmatrix}_{k \times k} \quad (9)$$

where the operator \odot means to determine whether the two-dimensional vectors are the same. Considering the accuracy of semantic segmentation, the semantic labels of two sets of correct correspondences may not necessarily match. Therefore, to reduce the reliance on semantic accuracy, we loosen the constraint of the semantic consistency by neighbor-based semantic consistency.

We search the neighbors $\mathcal{N}(\mathbf{p}_i)$ and $\mathcal{N}(\mathbf{q}_i)$ on the corresponding points \mathbf{p}_i and \mathbf{q}_i within a radius. Then, the semantic labels that have the highest proportion within the neighbor points are defined as $\mathcal{S}(\mathbf{p}_i)$ and $\mathcal{S}(\mathbf{q}_i)$. We calculate the neighbor-based semantic consistency matrix $\mathbf{M}'_s = [m_{ij}^{s'}]_{k \times k}$

$$m_{ij}^{s'} = (\mathcal{S}(\mathbf{q}_i), \mathcal{S}(\mathbf{q}_j)) \odot (\mathcal{S}(\mathbf{p}_i), \mathcal{S}(\mathbf{p}_j)). \quad (10)$$

We obtain the final semantic consistency matrix

$$\mathbf{M}_s^* = \mathbf{M}_s \otimes \mathbf{M}'_s \quad (11)$$

where operator \otimes represents the element-wise logical OR.

Finally, we embed semantic consistency into geometric consistency to get the semantic-geometric consistency

$$\mathbf{M}^* = \mathbf{M}_s^* \circ \mathbf{M}_g^*. \quad (12)$$

According to matrix \mathbf{M}^* , we apply the Top-k algorithm to filter out k_1 ($k_1 < k$) pairs of the correspondences for each set of local correspondences \mathcal{G}_l .

$$\mathcal{G}'_l = \left\{ \left((\mathbf{p}_n, s_n^p), (\mathbf{q}_n, s_n^q) \right) \mid n = \text{topk} \left(m_{lj}^* \right)_{j \in [1, k]} \right\} \quad (13)$$

After outlier removal, we get L groups of the filtered correspondences, and then we use SVD to get L candidate transformations.

$$\mathbf{R}_l, \mathbf{t}_l = \min_{\mathbf{R}, \mathbf{t}} \sum_{((\mathbf{p}_j, s_j^p), (\mathbf{q}_j, s_j^q)) \in \mathcal{G}'_l} w_j^l \|\mathbf{R}\mathbf{p}_j + \mathbf{t} - \mathbf{q}_j\|_2^2 \quad (14)$$

where w_j^l is the weight of inlier pair $(\mathbf{p}_j, \mathbf{q}_j)$ in correspondences \mathcal{G}'_l

$$w_j^l = m_{ij}^* / \sum_{j=1}^k m_{ij}^* \quad (15)$$

D. Two-Stage Hypothesis Verification

Traditional hypothesis verification based on inlier count often gets trapped in local optimality when encountering scenes with simple geometry and a large number of similar regions, leading to registration failure. To address this issue, we leverage the ground points $\mathbf{U}_{\mathbf{P}_g}$ segmented previously to perform ground normal verification, preemptively eliminating numerous local optimal solutions. Subsequently, we employ the truncation distance to select the optimal transformation $\tilde{\mathbf{T}}$. Therefore, we propose the two-stage verification for selecting transformation.

It can be seen from experience that in outdoor environments, within a certain distance, the normal direction of the ground plane remains consistent. In Section III-B, we obtained the ground point cloud by ground segmentation. As shown in Fig. 3, by using SVD, we obtain the normal

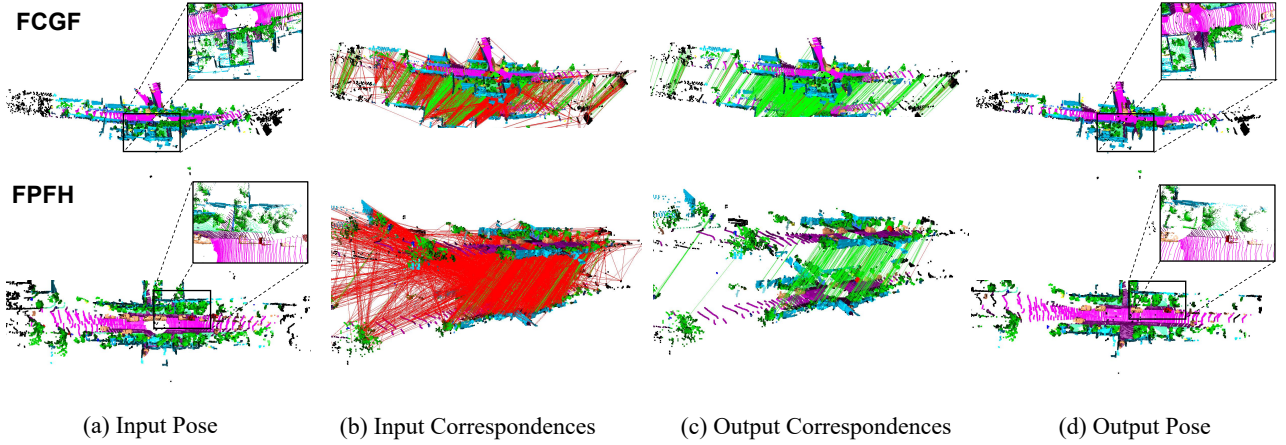


Fig. 4. Correspondences result and registration result on KITTI dataset.

vector \mathbf{n}_p of the ground which serves as a robust prior to guide the selection of candidate transformations

$$\mathbf{U}_p \Sigma_p \mathbf{V}_p^\top = \sum_{\mathbf{p}_i \in \mathbf{P}_g} (\mathbf{p}_i - \boldsymbol{\mu}) (\mathbf{p}_i - \boldsymbol{\mu})^\top \quad (16)$$

where \mathbf{P}_g is the ground part of the source point cloud and $\boldsymbol{\mu} = \frac{1}{|\mathbf{P}_g|} \sum_{\mathbf{p}_i \in \mathbf{P}_g} \mathbf{p}_i$. Ground normal \mathbf{n}_p can be calculated as $\mathbf{V}_p[:, -1]$. Similarly, the ground normal of the target point cloud is $\mathbf{n}_q = \mathbf{V}_q[:, -1]$. The wrong candidate transformations are eliminated by judging whether the candidate transformations can align two ground normal vectors,

$$|\cos(\mathbf{R}_l \mathbf{n}_p, \mathbf{n}_q)| < \sigma_\theta \quad (17)$$

where σ_θ is an angle threshold. After ensuring that there are no obviously wrong transformations, the best candidate transformation is selected by using the average truncation distance among the filtered global correspondences

$$\tilde{\mathbf{R}}, \tilde{\mathbf{t}} = \min_{\mathbf{R}_l, \mathbf{t}_l} \sum_{((\mathbf{p}_i, s_i^p), (\mathbf{q}_i, s_i^q)) \in \mathcal{G}'} TD(\mathbf{R}_l \mathbf{p}_i + \mathbf{t}_l, \mathbf{q}_i) \quad (18)$$

where $\mathcal{G}' = \mathcal{G}'_1 \cup \mathcal{G}'_2 \cup \dots \cup \mathcal{G}'_L$ and $TD(\cdot)$ is a truncated distance function, defined as

$$TD(\mathbf{p}_i, \mathbf{q}_i) = \begin{cases} 0.5\sigma_d, & \|\mathbf{p}_i - \mathbf{q}_i\|_2 \leq 0.5\sigma_d \\ \|\mathbf{p}_i - \mathbf{q}_i\|_2, & 0.5\sigma_d < \|\mathbf{p}_i - \mathbf{q}_i\|_2 < 2.5\sigma_d \\ 2.5\sigma_d, & 2.5\sigma_d \leq \|\mathbf{p}_i - \mathbf{q}_i\|_2 \end{cases} \quad (19)$$

E. Transformation Refinement

To further improve the accuracy of registration, the global correspondences \mathcal{G} are used to refine the transformation. We obtain the correspondences $\tilde{\mathcal{G}}$ that satisfies the best candidate transformation $\tilde{\mathbf{T}} = \{\tilde{\mathbf{R}}, \tilde{\mathbf{t}}\}$ on correspondences \mathcal{G}

$$\tilde{\mathcal{G}} = \left\{ ((\mathbf{p}_i, s_i^p), (\mathbf{q}_i, s_i^q)) \in \mathcal{G} \wedge \left\| \tilde{\mathbf{R}} \mathbf{p}_i + \tilde{\mathbf{t}} - \mathbf{q}_i \right\|_2 < \tau_1 \right\} \quad (20)$$

On correspondences $\tilde{\mathcal{G}}$, we use SVD again to achieve a more accurate transformation $\mathbf{T} = \{\mathbf{R}, \mathbf{t}\}$ of the global registration.

IV. EXPERIMENTS

A. Experimental Settings

1) *Benchmark Dataset*: We conduct experiments with both indoor and outdoor datasets. We have chosen the comprehensive KITTI dataset for outdoor scenes. Following [12]–[14], we conduct registration experiments on three sequences: 07, 08, and 09. In addition, we conduct indoor experiments on the 3DMatch dataset. Following [13], [14], we use 8 test scenes for evaluation.

2) *Evaluation Metric*: Following [13], [14], we evaluate the registration results by registration recall (RR), isotropic rotation error (RE), and L2 translation error (TE). Following [13], we consider registration as accurate when $RE < 5^\circ$ and $TE < 60$ cm for KITTI, and $RE < 15^\circ$ and $TE < 30$ cm for 3DMatch. For outlier removal, we adopt three evaluation metrics [13]: inlier precision (IP), inlier recall (IR), and F1-score (F1).

3) *Implementation Details*: The methods selected for experiments encompass the foremost outlier removal methods [11]–[14], [19], [30]–[32] as well as the most recent semantic-based registration methods [1], [16]. We implement methods [1], [33] under official guidelines. For other methods, following [13], [14], [20], we extract FPFH [28] and FCGF [29] descriptors and sample 8000 points with features as inputs. For KITTI, we directly predict semantics on point clouds by SalsaNext [15]. However, Utilizing RGBD images for semantic prediction is more suitable for indoor scenes. Hence, we employ RGBD data for semantic prediction by ESANet [34], which is then projected into a semantic point cloud. To ensure fairness, we set the input of other methods to the point cloud formed by a single image projection, rather than the point cloud reconstructed by TSDF [35].

B. Evaluation on KITTI odometry

Registration result. As demonstrated in Table I, we conduct comparative experiments with baselines [11]–[14], [19], [30]–[32] on the KITTI dataset. The algorithms above the dividing line are learning-based methods, while the latter ones are non-learning methods. Furthermore, the highlighted

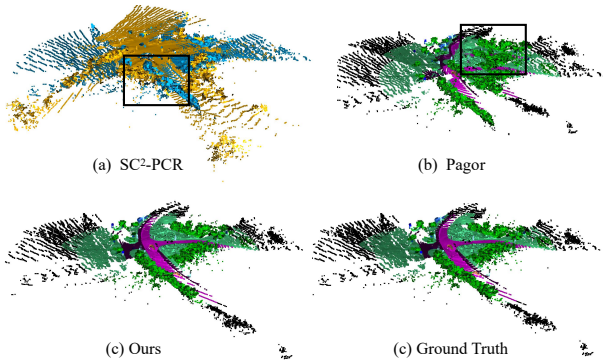


Fig. 5. Qualitative results under indistinct geometric features and few semantic categories. Despite the state-of-the-art method [13] and the semantic registration method [16] fail, our approach still achieves robust registration.

TABLE I
REGISTRATION RESULT ON KITTI DATASET.

Method	FPFH			FCGF			Time Sec.
	RR(\uparrow)	RE(\downarrow)	TE(\downarrow)	RR(\uparrow)	RE(\downarrow)	TE(\downarrow)	
DHVR [32]	-	-	-	98.20	0.47	20.54	3.91
DGR [19]	78.21	1.78	32.12	97.84	0.48	21.43	1.57
PointDSC [12]	97.12	0.59	8.98	97.48	0.47	20.76	0.30
VBReg [20]	96.04	0.70	15.29	98.20	0.46	20.32	0.33
SM [30]	77.66	0.63	13.22	96.22	0.63	21.27	0.08
RANSAC [11]	-	-	-	75.68	0.66	27.89	0.31
TEASER [31]	90.27	1.32	15.74	94.10	0.55	19.90	0.13
SC ² -PCR [13]	97.84	0.58	9.44	98.38	0.53	20.29	0.13
MAC [14]	98.20	0.60	8.71	98.38	0.48	20.19	1.32
Segregator [1]	70.12	1.52	18.81	-	-	-	0.14
Pagor [16]	76.39	0.91	17.25	-	-	-	0.08
SGOR (ours)	98.92	0.51	7.50	98.74	0.46	19.77	0.11

rows represent methods leveraging semantic information. “-” indicates the absence of results conducted under this specific condition in the official code. From Table I, it is evident that whether using FPFH or FCGF descriptors, our method achieves the most robust and accurate registration. Figure 4 (d) presents the visualization of the registration results obtained using our method. Compared with geometric-only methods [12]–[14], [31], our method introduces the fusion of semantic and geometric information, enabling more robust registration even in scenarios with indistinct geometric features, as shown in Fig. 5. Additionally, due to the verification with ground priors and semantic consistency, our registration exhibits lower TE and RE. Compared to the latest semantic registration methods [1], [16], our method shows significant improvement, with RR increasing from 76.39% to 98.92%, and RE and TE decreasing from 0.71 and 17.25 to 0.51 and 7.50, respectively. Moreover, the running time of our method is relatively short, only 0.11s for 8000 correspondences.

Correspondences result. In addition to robust and accurate registration, our method offers another advantage: the ability to filter out correspondences. When using the FPFH descriptors, our method outperforms in the outlier removal. As shown in Table II, it achieves 92.70% in IP and 94.59% in IR, indicating that while effectively filtering out the majority of outliers, we manage to retain almost all correct correspondences. However, for the learning-based FCGF descriptors, the learning-based method VBReg [20] achieves the best

TABLE II
CORRESPONDENCES RESULT ON KITTI DATASET.

Method	FPFH			FCGF		
	IP(\uparrow)	IR(\uparrow)	F1(\uparrow)	IP(\uparrow)	IR(\uparrow)	F1(\uparrow)
DGR [19]	78.39	54.12	62.15	72.19	78.06	75.13
PointDSC [12]	85.35	81.08	82.82	81.25	89.94	85.01
VBReg [20]	91.68	92.19	91.88	95.31	96.84	96.05
SM [30]	40.05	93.98	53.58	93.34	15.13	23.52
RANSAC [11]	2.09	15.72	3.58	57.90	80.12	65.89
TEASER [31]	82.56	68.08	73.98	73.02	67.99	69.05
SC ² -PCR [13]	90.07	92.75	91.27	82.50	91.52	86.37
SGOR (ours)	92.70	94.59	93.53	83.10	91.56	86.79

performance. Still, our method shows significant improvement compared to non-learning methods [13]. As qualitative results are shown in Fig. 4, our method accurately selects correct correspondences even in cases with a high percentage of outliers, ultimately achieving precise registration.

C. Evaluation on 3DMatch

TABLE III
QUALITATIVE RESULT ON 3DMATCH.

Method	FPFH					
	RR(\uparrow)	RE(\downarrow)	TE(\downarrow)	IP(\uparrow)	IR(\downarrow)	F1(\downarrow)
PointDSC [12]	45.78	2.82	8.53	38.46	40.17	38.87
VBReg [20]	55.70	3.17	9.42	46.33	49.93	47.69
SM [30]	31.25	4.10	11.09	28.11	51.84	32.24
RANSAC [11]	6.41	6.41	15.24	5.30	34.06	8.54
SC ² -PCR [13]	60.81	2.94	8.83	51.26	57.27	53.74
SGOR (ours)	65.01	2.51	9.02	55.12	55.90	55.51

Qualitative results. To evaluate the generalization ability of our approach, we conduct experiments on indoor scenes, and the results are presented in Table III. It is worth noting that these experiments are performed using the point clouds made by a single depth map, which typically exhibit incomplete geometric structures and low overlap, leading to overall performance inferior to that reported in [13], [14]. Table III demonstrates that our SGOR method outperforms SC2-PCR [13] in terms of RR by using FPFH descriptors, with improvements of 4.2 pp. This enhancement is attributed to our method’s ability to effectively address challenges such as incomplete geometry and low overlap, resulting in more robust registration. Furthermore, our approach also performs well in outlier removal on the 3DMatch dataset. Compared to SC2-PCR [13], our method achieves higher IP, indicating superior outlier filtering capabilities.

D. Robustness Test

Robustness to different thresholds. Different tasks have different error requirements. We conduct a robustness test by applying three distinct error thresholds: easy (5° , 60cm), medium (5° , 30cm), and hard (2° , 10cm). The results, as shown in Table IV, indicate that our method achieves the highest success rate under all three different conditions. Specifically, under the strict criteria of $RE < 2^\circ$ and $TE < 10$ cm, our method still achieves a 76.40% success rate.

TABLE IV
ROBUSTNESS TEST UNDER DIFFERENT ERROR THRESHOLDS.

Method	FPFH			FCGF		
	easy	medium	hard	easy	medium	hard
PointDSC [12]	97.12	95.14	<u>67.03</u>	97.48	74.59	<u>23.06</u>
VBReg [20]	96.04	88.65	27.75	98.20	75.68	22.52
RANSAC [11]	-	-	-	75.68	43.78	6.49
SM [30]	77.66	69.73	39.28	96.22	<u>76.04</u>	23.60
SC ² -PCR	97.84	96.94	59.82	<u>98.38</u>	75.32	<u>23.06</u>
Segregator [1]	70.12	54.10	10.68	-	-	-
Pagor [16]	76.39	58.01	9.18	-	-	-
SGOR (<i>ours</i>)	98.92	97.66	76.40	98.74	77.66	23.60



Fig. 6. (a): Registration Recall under different numbers of correspondences; (b): Registration Recall under different semantic conditions.

Robustness to correspondence quantity. We conduct random sampling of correspondences to get different numbers of correspondences. As shown in Fig. 6 (a), SC2-PCR [13] shows a significant decrease in RR with too many or too few correspondences. PointDSC [12] fails to achieve robust registration when there are fewer correspondences. In contrast, our method exhibits good robustness to the number of correspondences and maintains high performance.

Robustness to semantic label quantity. As shown in Fig. 6 (b), according to the number of effective semantic categories, we divide the KITTI dataset into four types. when the number of semantic categories decreases, the most advanced semantic-based method [16] experiences a significant decrease in RR, dropping from 90% to 36%. In contrast, our method consistently maintains a high level of performance even when poor semantics like Fig. 5.

Robustness to semantic label quality. We further validate the robustness of our method to semantic quality through experiments. To simulate poor semantic prediction, we randomly substitute semantic labels for 50% points in the point cloud. Under this condition, our method is compared with Pagor [16] and Segregator [1]. After noise experiments, our approach achieves a 91.21% RR in the high-noise scenarios. Compared to the original decrease of only 7.61 pp, our method exhibits a much lower decline than Pagor’s decrease of 42.90 pp and Segregator’s decrease of 15.09 pp.

E. Ablation Study

In this section, we conduct ablation experiments on the KITTI dataset to validate the effectiveness of individual modules. The experimental results are presented in Table V where * indicates the default settings of our SGOR.

Preprocessing of correspondences. We perform preprocessing of correspondences, involving the filtering of ground

points and estimation of potential overlapping regions. A comparison between methods No.1 and 2 clearly demonstrates that, with correspondence preprocessing, our approach achieves a significant improvement in RR and a reduction in registration errors. Furthermore, due to filtering many useless points, the processing speed is improved.

Secondary ground segmentation. The plane segmentation module is essential to our approach. Its accuracy will directly affect the feature matching and candidate transformation screening. We use the simple plane estimation only by predicted semantics to replace the secondary ground segmentation. As can be seen from rows No.3, and 4 in Table V, the performance of the ablation model has been significantly diminished, which illustrates the importance of our plane segmentation method.

Using Semantic information. From rows No.5, and 7 in Table V, it is evident that incorporating semantic-geometric information into the geometric-only method yields noticeable improvements, increasing RR from 91.35%/97.66% to 98.92%/98.74%. The results underscore the significance and effectiveness of our semantic-geometric method. To further highlight the superiority of our loose regional semantic consistency, we replace it with a strict point-to-point semantic consistency like [16]. It can be seen from Table V (6) and (7) that our method reduces the dependence on semantic accuracy and achieves more accurate and robust registration.

Two-stage verification. We have enhanced the hypothesis verification for ground verification, utilizing the point cloud of the ground with indistinct features. As demonstrated in experiments No. 8 and 9, it is evident that this ground verification makes our method more robust, improving RR by 13.01%.

TABLE V
ABLATION STUDY ON KITTI DATASET.

No.	Methods	FPFH			FCGF		
		RR(↑)	RE(↓)	TE(↓)	RR(↑)	RE(↓)	TE(↓)
1)	W/o preprocessing of correspondences	89.01	0.55	9.32	97.48	0.54	20.29
2)	W/ preprocessing of correspondences*	98.92	0.51	7.50	98.74	0.46	19.77
3)	Ground segmentation only by semantics	90.21	0.67	9.25	97.14	0.75	20.00
4)	Secondary ground segmentation*	98.92	0.51	7.50	98.74	0.46	19.77
5)	Geometric-only SGOR	91.35	0.53	9.34	97.66	0.51	20.26
6)	Semantic-hard SGOR	95.81	0.63	9.41	95.78	0.69	21.00
7)	Semantic-geometric SGOR*	98.92	0.51	7.50	98.74	0.46	19.77
8)	Verification without ground prior	85.91	0.57	9.97	96.90	0.62	20.26
9)	Two-stage verification*	98.92	0.51	7.50	98.74	0.46	19.77

V. CONCLUSION

This paper presents a novel method for outlier removal that leverages semantic information. This method effectively filters out erroneous correspondences, resulting in a significantly more robust and accurate registration. By harnessing semantic information and ground priors of outdoor scenes, we address the challenge of incorrect correspondences and registration failures in difficult scenarios marked by indistinct features and few semantic labels. In our future work, we intend to develop a lightweight network for extracting both semantics and features to cooperate with our SGOR.

REFERENCES

- [1] P. Yin, S. Yuan, H. Cao, X. Ji, S. Zhang, and L. Xie, "Segregator: Global point cloud registration with semantic and geometric cues," in *2023 IEEE International Conference on Robotics and Automation (ICRA)*, 2023, pp. 2848–2854.
- [2] C. Zhang, H. Zhao, C. Wang, X. Tang, and M. Yang, "Cross-modal monocular localization in prior lidar maps utilizing semantic consistency," in *2023 IEEE International Conference on Robotics and Automation (ICRA)*, 2023, pp. 4004–4010.
- [3] P. Vial, M. Malagón, R. Segura, N. Palomeras, and M. Carreras, "Gmm registration: a probabilistic scan matching approach for sonar-based auv navigation," in *2023 IEEE International Conference on Robotics and Automation (ICRA)*, 2023, pp. 1033–1039.
- [4] J. Ruan, B. Li, Y. Wang, and Y. Sun, "Slamesh: Real-time lidar simultaneous localization and meshing," in *2023 IEEE International Conference on Robotics and Automation (ICRA)*, 2023, pp. 3546–3552.
- [5] M. Gentner, P. Kumar Murali, and M. Kaboli, "Gmcr: Graph-based maximum consensus estimation for point cloud registration," in *2023 IEEE International Conference on Robotics and Automation (ICRA)*, 2023, pp. 4967–4974.
- [6] J. Chao, S. Enginl, N. Häni, and V. Isler, "Category-level global camera pose estimation with multi-hypothesis point cloud correspondences," in *2023 IEEE International Conference on Robotics and Automation (ICRA)*, 2023, pp. 3800–3807.
- [7] M. Yuan, X. Huang, K. Fu, Z. Li, and M. Wang, "Boosting 3d point cloud registration by transferring multi-modality knowledge," in *2023 IEEE International Conference on Robotics and Automation (ICRA)*, 2023, pp. 11 734–11 741.
- [8] H. Yu, F. Li, M. Saleh, B. Busam, and S. Ilic, "Cofinet: Reliable coarse-to-fine correspondences for robust pointcloud registration," *Advances in Neural Information Processing Systems*, vol. 34, pp. 23 872–23 884, 2021.
- [9] G. Chen, M. Wang, Q. Zhang, L. Yuan, T. Liu, and Y. Yue, "Deep interactive full transformer framework for point cloud registration," in *2023 IEEE International Conference on Robotics and Automation (ICRA)*, 2023, pp. 2825–2832.
- [10] S. Huang, Z. Gojic, M. Usvyatsov, A. Wieser, and K. Schindler, "Predator: Registration of 3d point clouds with low overlap," in *Proceedings of the IEEE/CVF Conference on computer vision and pattern recognition*, 2021, pp. 4267–4276.
- [11] M. A. Fischler and R. C. Bolles, "Random sample consensus: a paradigm for model fitting with applications to image analysis and automated cartography," *Communications of the ACM*, vol. 24, no. 6, pp. 381–395, 1981.
- [12] X. Bai, Z. Luo, L. Zhou, H. Chen, L. Li, Z. Hu, H. Fu, and C.-L. Tai, "Pointsc: Robust point cloud registration using deep spatial consistency," in *Proceedings of the IEEE/CVF Conference on Computer Vision and Pattern Recognition*, 2021, pp. 15 859–15 869.
- [13] Z. Chen, K. Sun, F. Yang, and W. Tao, "Sc2-pcr: A second order spatial compatibility for efficient and robust point cloud registration," in *Proceedings of the IEEE/CVF Conference on Computer Vision and Pattern Recognition*, 2022, pp. 13 221–13 231.
- [14] X. Zhang, J. Yang, S. Zhang, and Y. Zhang, "3d registration with maximal cliques," in *Proceedings of the IEEE/CVF Conference on Computer Vision and Pattern Recognition*, 2023, pp. 17 745–17 754.
- [15] T. Cortinhal, G. Tzelepis, and E. Erdal Aksoy, "Salsanext: Fast, uncertainty-aware semantic segmentation of lidar point clouds," in *Advances in Visual Computing: 15th International Symposium, ISVC 2020, San Diego, CA, USA, October 5–7, 2020, Proceedings, Part II 15*. Springer, 2020, pp. 207–222.
- [16] Z. Qiao, Z. Yu, H. Yin, and S. Shen, "Pyramid semantic graph-based global point cloud registration with low overlap," *arXiv preprint arXiv:2307.12116*, 2023.
- [17] K. G. Derpanis, "Overview of the ransac algorithm," *Image Rochester NY*, vol. 4, no. 1, pp. 2–3, 2010.
- [18] Q.-Y. Zhou, J. Park, and V. Koltun, "Fast global registration," in *Computer Vision—ECCV 2016: 14th European Conference, Amsterdam, The Netherlands, October 11–14, 2016, Proceedings, Part II 14*. Springer, 2016, pp. 766–782.
- [19] C. Choy, W. Dong, and V. Koltun, "Deep global registration," in *Proceedings of the IEEE/CVF conference on computer vision and pattern recognition*, 2020, pp. 2514–2523.
- [20] H. Jiang, Z. Dang, Z. Wei, J. Xie, J. Yang, and M. Salzmann, "Robust outlier rejection for 3d registration with variational bayes," in *Proceedings of the IEEE/CVF Conference on Computer Vision and Pattern Recognition*, 2023, pp. 1148–1157.
- [21] G. Zhao, Z. Du, Z. Guo, and H. Ma, "Vrhcf: Cross-source point cloud registration via voxel representation and hierarchical correspondence filtering," *arXiv preprint arXiv:2403.10085*, 2024.
- [22] Z. Qin, H. Yu, C. Wang, Y. Guo, Y. Peng, and K. Xu, "Geometric transformer for fast and robust point cloud registration," in *Proceedings of the IEEE/CVF Conference on Computer Vision and Pattern Recognition*, 2022, pp. 11 143–11 152.
- [23] T. Brown, B. Mann, N. Ryder, M. Subbiah, J. D. Kaplan, P. Dhariwal, A. Neelakantan, P. Shyam, G. Sastry, A. Askell, et al., "Language models are few-shot learners," *Advances in neural information processing systems*, vol. 33, pp. 1877–1901, 2020.
- [24] A. Kirillov, E. Mintun, N. Ravi, H. Mao, C. Rolland, L. Gustafson, T. Xiao, S. Whitehead, A. C. Berg, W.-Y. Lo, et al., "Segment anything," *arXiv preprint arXiv:2304.02643*, 2023.
- [25] D. Menini, S. Kumar, M. R. Oswald, E. Sandström, C. Sminchisescu, and L. Van Gool, "A real-time online learning framework for joint 3d reconstruction and semantic segmentation of indoor scenes," *IEEE Robotics and Automation Letters*, vol. 7, no. 2, pp. 1332–1339, 2021.
- [26] S.-S. Huang, H. Chen, J. Huang, H. Fu, and S.-M. Hu, "Real-time globally consistent 3d reconstruction with semantic priors," *IEEE transactions on visualization and computer graphics*, 2021.
- [27] X. Chen, A. Milioto, E. Palazzolo, P. Giguere, J. Behley, and C. Stachniss, "Suma++: Efficient lidar-based semantic slam," in *2019 IEEE/RSJ International Conference on Intelligent Robots and Systems (IROS)*. IEEE, 2019, pp. 4530–4537.
- [28] R. B. Rusu, N. Blodow, and M. Beetz, "Fast point feature histograms (fpfh) for 3d registration," in *2009 IEEE international conference on robotics and automation*. IEEE, 2009, pp. 3212–3217.
- [29] C. Choy, J. Park, and V. Koltun, "Fully convolutional geometric features," in *2019 IEEE/CVF International Conference on Computer Vision (ICCV)*, 2019, pp. 8957–8965.
- [30] M. Leordeanu and M. Hebert, "A spectral technique for correspondence problems using pairwise constraints," in *Tenth IEEE International Conference on Computer Vision (ICCV'05) Volume 1*, vol. 2. IEEE, 2005, pp. 1482–1489.
- [31] H. Yang, J. Shi, and L. Carlone, "Teaser: Fast and certifiable point cloud registration," *IEEE Transactions on Robotics*, vol. 37, no. 2, pp. 314–333, 2020.
- [32] J. Lee, S. Kim, M. Cho, and J. Park, "Deep hough voting for robust global registration," in *Proceedings of the IEEE/CVF International Conference on Computer Vision*, 2021, pp. 15 994–16 003.
- [33] Z. Qiao, Z. Yu, B. Jiang, H. Yin, and S. Shen, "G3reg: Pyramid graph-based global registration using gaussian ellipsoid model," *arXiv preprint arXiv:2308.11573*, 2023.
- [34] D. Seichter, M. Köhler, B. Lewandowski, T. Wengefeld, and H.-M. Gross, "Efficient rgb-d semantic segmentation for indoor scene analysis," in *2021 IEEE international conference on robotics and automation (ICRA)*. IEEE, 2021, pp. 13 525–13 531.
- [35] A. Zeng, S. Song, M. Nießner, M. Fisher, J. Xiao, and T. Funkhouser, "3dmatch: Learning local geometric descriptors from rgb-d reconstructions," in *Proceedings of the IEEE conference on computer vision and pattern recognition*, 2017, pp. 1802–1811.